Conceptual Study of Counter-Rotating Turbofan Engines

Conference Paper · October 2010

DOI: 10.1115/GT2010-22770

3 authors:

Néstor González Díez
TNO
20 PUBLICATIONS **49** CITATIONS
SEE PROFILE

Arvind Gangoli Rao
Delft University of Technology
86 PUBLICATIONS **928** CITATIONS
SEE PROFILE

Jos P. van Buijtenen
Triogen B.V., The Netherlands
72 PUBLICATIONS **367** CITATIONS
SEE PROFILE

Proceedings of ASME Turbo Expo 2010: Power for Land, Sea and Air
GT2010
June 14-18, 2010, Glasgow, UK

GT2010-22770

CONCEPTUAL STUDY OF COUNTER-ROTATING TURBOFAN ENGINES

Néstor González Díez **Arvind G. Rao*** **Jos van Buijtenen**

Faculty of Aerospace Engineering
Delft University of Technology, The Netherlands

ABSTRACT

The dramatic growth that air traffic has experienced in the last years is not likely to slow down in the future. The situation for the airlines has however been critical due to the large share of the operating costs corresponding to fuel. On the other hand, the society demands quieter aircraft which is then translated into stricter regulations. The Advisory Council for Aeronautics Research in Europe (ACARE) has set an ambitious array of objectives to be accomplished by 2020. It is often claimed that complying with those targets will not require evolution but, rather, revolution.

One of the potential future engine configurations being considered is the counter-rotating turbofan (CRTF) concept. This paper addresses the possibilities of improvement that the CRTF can offer with respect to the specific fuel consumption, emissions and noise as compared to the baseline engine, the GE90. Semi-empirical correlations and methodologies have been used for the study. First a Blade Element Method (BEM) is developed to estimate the performance of the fan and to build confidence upon the applied loss and deviation angle models. Next, the design methodology is applied to three cases: a single-stage fan featuring the reference properties of the GE90 engine; a counter-rotating fan (CRF) fan with similar properties as a GE90 fan, but with a lower rotational speed; and a CRF with higher fan pressure ratio (FPR) for lower specific fuel consumption. Finally, noise emission by all the three configurations are estimated by noise models available in the literature.

Reductions of equivalent perceived noise level (EPNL) were found to be possible if a CRF is used instead of the baseline single-stage arrangement. Other noise descriptors are also reduced by a similar amount. Approximately equal noise levels are expected if the CRF is of higher pressure than the baseline.

Keywords: Aero Engine, Aircraft propulsion, Blade Element Method, Counter-rotating fan, Engine Noise

* Corresponding Author, a.gangolirao@tudelft.nl
Tel:- +31-152783833

NOMENCLATURE

a	Constant used in vortex design
B	Number of rotor blades
b	Constant used in vortex design
f	Frequency
$\dot{m}$	Mass flow
M	Mach number
M_{tr}	Tip relative Mach number
n	Tailoring exponent for the vortex design
r	Radius measured from the engine axis
T_0	Total (or stagnation) temperature
V	Number of stator vanes

Greek Symbols

κ	Metal angle
θ	Polar angle
β	Bypass Ratio

Acronyms

AVR	Axial-Velocity Ratio
BPF	Blade Passing Frequency
BPR	Bypass Ratio
BR	Back rotor of a CRF
CRF	Counter-Rotating Fan
CRT	Counter-rotating turbine
CRTF	Counter-Rotating Turbofan
EPNL	Equivalent Perceived Noise Level
FPR	Fan Pressure Ratio
FR	Front rotor of a CRF
IGV	Inlet guide vanes
OASPL	Overall A-weighted Sound Pressure Level
SPL	Sound Pressure Level
TPNL	Tone-corrected Perceived Noise Level
TSFC	Thrust Specific Fuel Consumption

1. INTRODUCTION

The current global economy is assisted to a large extent by aviation. Consequently, this has represented the flourishing and uprising of many new airlines, as well as increases in operations for the traditional ones. In parallel to it, several problems have arisen. The oil price during this decade followed, until 2008, a steady rise reaching levels equivalent to those of the oil crisis in the seventies. The share of the operating costs associated to fuel has come to values over 25% in 2007 (see figure 1), strongly affecting their economics. Environmental implications of the air traffic growth are also of concern in terms of pollutant emissions (CO_2 and NO_x), as well as noise footprints in the vicinity of the airports. The Advisory Council for Aeronautics Research in Europe (ACARE) has compiled a set of goals to be accomplished by 2020 (Vision20). Challenges such as halving the perceived noise levels and the CO_2 emissions as well as reductions of 80% in NO_x are part of the vision. The propulsion system is largely responsible of such issues. Incremental evolutions in current engines will not be sufficient to meet these future regulations, and thus a step change is needed.

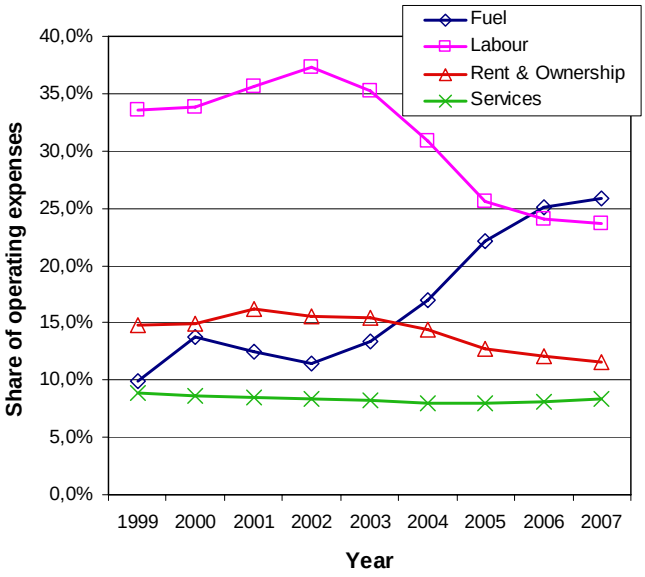

Figure 1 - Evolution of shares of operating costs. Data from Air Transport Association [1].

1.1 Towards cleaner engines

Large reductions in fuel consumption have been achieved by increasing the thermodynamic cycle efficiency and the propulsive efficiency. Whereas the first depends mostly on the turbine thermal endurance (materials and cooling) and component efficiencies, the second can be increased by increasing the bypass ratio (BPR). Over the years, the BPR of turbofan engines has been increasing and has been one of the main sources for reduction in the specific fuel consumption (SFC) of the engines; however the BPR can not be increased perpetually due to several practical problems which include increasing fan diameter (that increases fan weight) and reducing ground clearance. Also, large diameters fans run at lower shaft speeds in order to avoid important compressibility effects in the fan. The variation of the specific fuel consumption with fan pressure ratio (FPR) for various BPR is shown in Fig. 2. It can be seen that for a given BPR, there is an optimum FPR at which the engine SFC is minimum.

Reducing the fuel consumption goes hand in hand with reductions in CO_2 emissions for hydrocarbon based fuels. The CO_2 emissions could be also decreased by using alternative fuels, e.g. those with lower carbon footprint (biofuels) or liquid hydrogen. The NO_x emission depends mainly on the combustor technology. Noise exposure has been tremendously lowered since the beginning of the turbofan age in aviation.

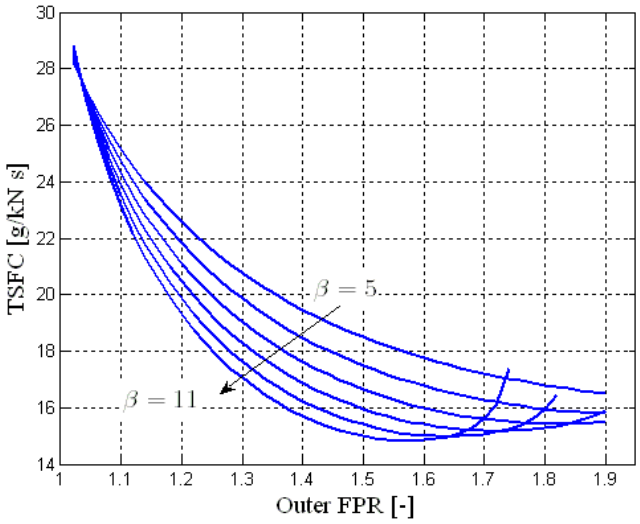

Figure 2 – Specific fuel consumption Vs BPR and FPR for a Turbofan engine.

The current necessity for a revolution in the propulsion plant demands the engine manufacturers to investigate novel propulsion concepts. The Geared Turbofan concept introduces a gearbox in the low-pressure shaft to decouple the rotational motion of the fan and the turbine, hence enabling higher BPR (and lower FPR) capabilities. The Intercooled Recuperated Aeroengine concept takes advantage of the heat present in the exhaust gas by looping it back to the combustor inlet, so that the cycle thermal efficiency is increased. Finally, a return to the open-rotor propfans is visible in the long term due to the fact that much lower fuel consumptions are attained. However, it remains unclear whether the inherent inability to shield the noise generated by the rotor in a very noise stringent

scenario will put a wall to their development. Other certification issues such as rotor blade off containment still remain an issue.

1.2 The Counter-Rotating Fan concept

Another propulsion concept put forward is Counter-Rotating Turbofan (CRTF). This engine is being studied by Snecma within the EnVIronmenTALly Friendly Aero Engines (VITAL) project framework [2]. It features a two-stage counter-rotating fan (CRF) in the front part of the engine, instead of a common single-stage fan (see figure 3). These two stages allow a split in the total aerodynamic load of the fan stage. Two design philosophies are foreseen. First, a reduction in tip speed is possible if it is decided to keep the FPR and the BPR constant for the same net thrust and size. A second possibility is reducing the size of the fan to obtain benefits in terms of weight and drag, although it goes with an increase in FPR to keep the same thrust. This could lead to a slight decrease in propulsive efficiency. The benefits of a smaller engine would need to be carefully analysed for a particular aircraft and its mission to check whether they compensate for the increase in TSFC.

There are mainly two options for the drive of the CRF: a gearbox or a counter-rotating turbine (CRT). The use of a gearbox initially adds weight to the engine. However, the turbine can be designed optimally, potentially enabling a lower number of stages and redressing to a certain extent for the gearbox weight. Implementing a CRT might as well reduce the overall turbine section weight, but it requires a triple spool configuration. The much larger relative speed between the shafts can cause some maintenance problems and inferior mechanical efficiency.

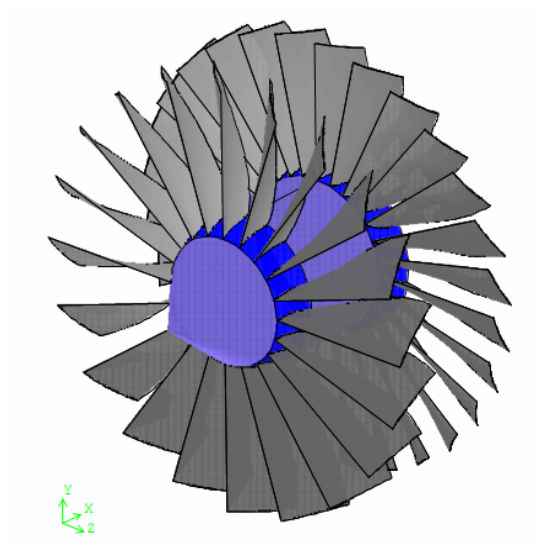

Figure 3 – Schematic of a counter-rotating fan.

2. METHODOLOGY

In order to assess the feasibility of the counter-rotating turbofan (CRTF) concept it was compared against a reference engine. The GE90 engine was chosen as the baseline engine in this respect.

The outline of the present analysis can be found in figure 4. First, the *analysis problem* is addressed with the help of the Blade Element Method. An implementation is done to estimate the performance of turbomachinery rows, and hence be able to validate the calculation procedures. Later, the task is reversed into the *design problem*, which is applied for the design point of the reference engine and for the CRTF concepts. Next, an implementation of source models obtained from the literature is performed to be able to calculate the radiated noise spectra due to the fan. Finally, some noise descriptors are found for a take-off operation according to the International Civil Aviation Organization (ICAO) regulations.

2.1 Blade Element Method (BEM):

The performance of an axial fan or compressor can be estimated by making use of the BEM. It consists of the discretization of the blade into a number of annuli from hub to tip for which the velocity triangles and the efficiency have to be estimated. The input information for a solver based on the BEM is the detailed geometry of the blade and the operating conditions (altitude as well as shaft rotational speed). The result is the complete determination of the aero-thermodynamic state of the air at the exit of the blade row. Several difficulties have to be overcome when applying the BEM-based solver at the fan design point: the determination of the deviation angle, the axial velocity variation across the blade, and the losses.

The deviation angle is defined as the angle between the exit air angle and the trailing edge airfoil (or metal) angle. This difference exists due to the boundary layer growth over the suction side of the airfoil. The consequence is that the performance is lower than expected if the air was expected to smoothly follow the blade profile. Several rules exist based on experimental studies and correlations. In the present analysis, the method of Lieblein [3] is employed. This method is a refined version of the historically widely used Carter's rule.

The axial velocity ratio (AVR) is calculated from the solution of the non-isentropic radial equilibrium equation after neglecting the radial acceleration term, as pointed out in [4].

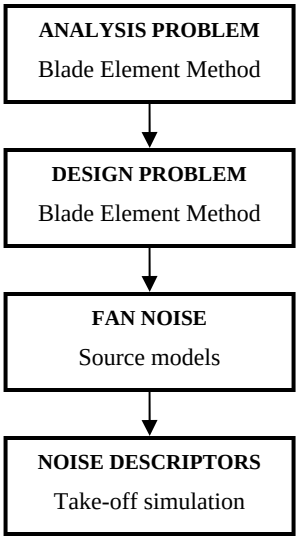

Figure 4 – Methodology outline for the present study.

The blade losses considered are composed of the profile losses, the end-wall and secondary flow losses and the shock losses. All of them were estimated from the analysis of a modified diffusion factor which takes into account the compressibility effects. The magnitude of the loss coefficient is then interpolated from the correlations presented in [5].

An assessment of the validity of the aspects explained above was undertaken by comparing the results with two reference rotor, NASA's rotor 55 [6] and NASA's rotor 57 [7]. Spanwise results at the design point and maps were generated. The last are shown in figure 5. For the rotor 55, the performance was slightly overestimated at the three levels of rotational speed for which experimental data were available. It was found that in this case an equivalent overestimation was being calculated for the temperature ratio map, which was caused by predicting more diffusion across the blade than experimentally indicated. For the rotor 57, the calculated lines are in close agreement with the experimental results up to the point in which the rotational speed reaches transonic and supersonic values (at 100, 110 and 120%). From the spanwise results it was checked that this was due to a miscalculation of the deviation angle. Lieblein's method is feasible only at moderate speeds. Despite this realisation, further stages of this study still make use of this method, although it is acknowledged that correlations for transonic regimes should be implemented instead.

The blade element method may also be used in the reversed or *design problem* in order to find a specific shape for a desired aerodynamic performance. One of the degrees of freedom at the design point is given by the incidence angle by selecting an appropriate leading edge metal angle. In the present study, this selection was the result of calculating the minimum-loss incidence angle, according to the method exposed in [3]. Another degree of freedom when designing axial turbomachinery is the vortex design, i.e. the profile of tangential velocity $C_{\theta,2}$ at the blade trailing edge. It has to be imposed according to the needs and limitations imposed by the diffusion factor. In the present study, arbitrary distributions based on the tailoring exponent *n* were evaluated:

$$C_{\theta,2} = \frac{a}{r} + b\, r^{n} \qquad (1)$$

where *a* and *b* are constants, and *r* is the radius from the engine axis. The exponent was always chosen such that the work done increases towards the tip of the blade. Several assumptions and limitations were present in the design phase. First, due to the availability of the correlations previously presented, the solidity was limited to a maximum value of 2. This is in contrast with the modern fan design practice, in which values of 3 or higher are known to be used at the near-hub region [8]. The blade airfoils were assumed as double circular arcs (DCA) throughout its full span, for the sake of simplicity regarding geometrical relations between the metal angles. It is recognised that other airfoils (NACA series) would be better used in the purely subsonic region. The thickness distribution was always assumed to follow a linear relation featuring 3 % at the tip and 12 % at the hub.

The design process was adapted to the CRTF concept by simply applying it in series. This means that the aerothermodynamic state of the air at the exit of the front rotor is directly the inflow state for the back rotor. The spacing between the two rotors was not captured in the design methodology, and therefore is not considered at this stage.

2.2 Fan Noise:

The estimation of the noise generated by the fan was undertaken by making use of semi-empirical based methods. These are the method by Heidmann [9] and the method endorsed by the Engineering Society of Data Units (ESDU, [10]). The application of these methods gives, as a result, the spectrum of the fan noise at any polar angle from the engine axis radiated from the inlet or the exhaust. The spectrum is calculated by evaluating the 1/3-octave bands central frequency. The sound pressure level (SPL) consists of a broadband contribution and a tonal contribution. In the case that the relative Mach number at the tip is supersonic,

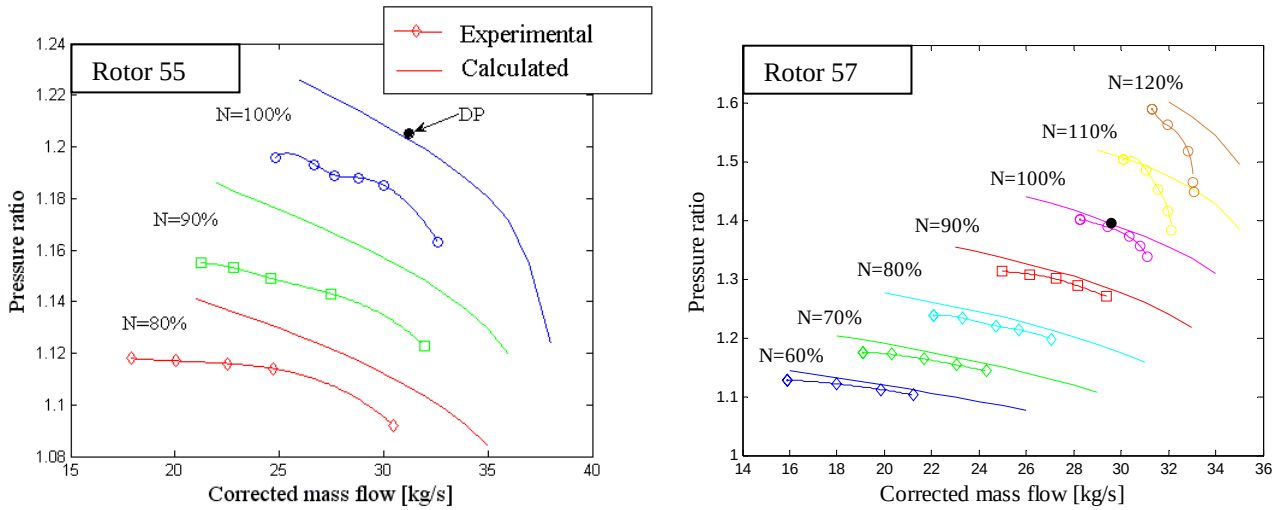

Figure 5 – Fan map estimation and experimental results for rotor 55 and rotor 57

shock noise is also taken into account. There are a number of circumstances that must be also taken into account: ground roll operation as opposed to flight conditions, first or second fan stage, and the presence of inlet guide vanes (IGV).

Heidmann's and ESDU's methods rely upon the correlation shown below, in which the rise in total temperature and the mass flow through the fan are important. The rest of the terms depend on the specific design of the fan: its design and relative tip Mach number (M_{tr}), i.e. the Mach number of the blade tip due to its tangential and axial motion with respect to the air; the rotor-stator spacing (RSS), which is the relation between the spacing and the chord of the blade; and the blade passing frequency (BPF), through the blade and vane count.

$$SPL(f,\theta) = 20\log_{10}(\Delta T_t) + 10\log_{10}(\dot{m}) + F_1(M_{tr}) + \\ + F_2(RSS) + F_3(\theta) + F_4(f/BPF) + C \qquad (2)$$

It is clear from this formula that given a certain FPR, the noise generated is less if the total temperature rise necessary to achieve the pressure rise is less, i.e. the efficiency is higher. The temperature rise term is also the only one in which the detailed geometry of the blade is represented, as it influences the efficiency. Unfortunately, modern techniques proven to further reduce noise such as lean and sweep are by no means captured in these methods.

The discrete tone noise is calculated from a fundamental tone level in a similar fashion. This fundamental tone level can be reduced if the cut-off condition (eq. 3) is satisfied,

$$\frac{M_{tr}}{1 - V/B} < 1.05 \qquad (3)$$

with M_{tr} the relative tip Mach number, V the number of stator vanes and B the number of rotor blades. This condition follows from the theory of Tyler and Sofrin [11]. The magnitude of the reduction depends on the method used for the evaluation.

2.3 Noise descriptors and measurements.

The source models for the fan, once implemented, can be used to obtain other noise descriptors for a take-off event. This is motivated by the fact that regulations and health recommended values are expressed in terms of these descriptors. The steps to make such estimation are outlined in figure 6 .

In the take-off simulation, first the distance between the aircraft engine and the noise measurement point under consideration is needed, and second, the relative angle between the engine axis and this point. This was performed according to the ICAO certification regulations [12]. The flight speed was chosen to be 15 knots over the climbout safety speed. The flyover measurement point is located at 6500 m on the extended centreline of the runway from the start of the take-off roll. The lateral noise measurement point lied at 450 m from the centerline point where the noise level was maximum during take-off.

The fan noise models were applied for the polar angle and distance recorded in the take-off simulation at every instant. The effects of atmospheric attenuation and ground

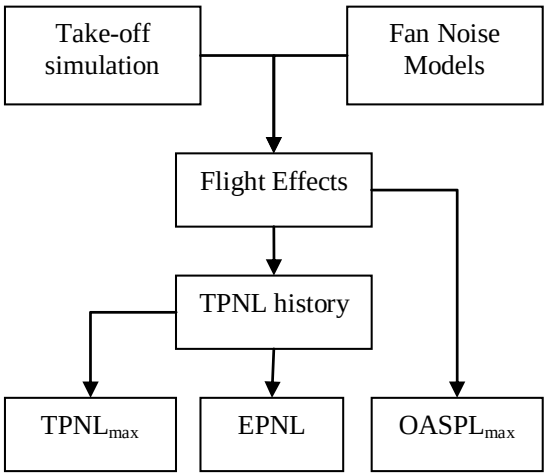

Figure 6 – Steps to find relevant noise descriptors.

reflection were not taken into account. Then, a correction for the flight effects was performed upon the spectrum obtained, as the perceived frequencies by an observer are different from those emitted at the source. The frequencies were corrected according by [13]

$$f_{flight} = \frac{f_{static}}{1 - M\ \cos\theta} \qquad (4)$$

The effects of forward motion are also present through the convection of the effective pressure, as measured at a certain static position. Due to the fact that we are considering only the noise generated by the fan, and this can be understood as the coalescence of several sources of dipolar nature, the SPL can be corrected with the next formula valid only for monopole/dipole sources:

$$SPL_M = SPL_{M=0} - 40\log_{10}\left(1 - M\ \cos\theta\right) \qquad (5)$$

It must be also noticed that due to the Doppler shift, the noise spectrum generated at the source is perceived differently and the same measurement (e.g. a tone) can travel between different 1/3-octave bands. So, in order to find the perceived spectrum at the standard band central frequencies, the SPL values are interpolated from the shifted spectrum on those frequencies. All the energy that, due to the shifting, is perceived beyond the 10 kHz limit is not rated. This process is shown in figure 7, in which the fan is travelling towards the measurement point, causing an increase in SPL and a shift towards higher frequencies.

The noise descriptors used in the present study are:

- Maximum tone-corrected perceived noise level ($TPNL_{max}$), giving an indication of the maximum level of annoyance reached at the measurement point.

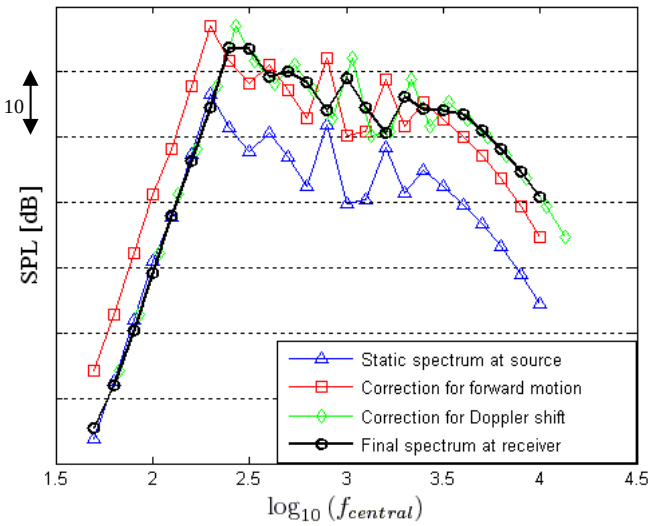

Figure 7 – Spectrum modification due to forward motion.

- Equivalent Perceived Noise Level (EPNL), which takes into account the duration of the take-off event.
- Maximum Overall A-weighted Perceived Noise Level ($OASPL_{max}$), providing an indication of the maximum loudness as perceived by a hypothetical human observer located at the measurement point.

In order to find the EPNL, the TPNL-history is necessary. At each time step, the TPNL can be found from the spectrum levels in 1/3-octave bands by transforming the levels into annoyance values (whose unit is the *noy*) to get the PNL and finding the correction to be applied due to the presence of tones. The EPNL is subsequently calculated. Finally, obtaining the $OASPL_{max}$ only requires correcting the spectrum for the specific human sensitivity to high frequencies and finding the overall value at each time step.

3. APPLICATION OF THE METHODOLOGY

Three fans were designed. The first one was a single stage fan that is used on the baseline engine; second, a CRF for the same FPR but lower rotational speed is attempted; and third, a CRF with a higher pressure ratio.

The cycle design point for the single stage fan was assumed at cruise conditions [14]. The relevant information for the fan design and a set of results of the application of the design tool are shown in table 1. The outer FPR requirement of 1.65 could not be reached with the current tool, so eventually a value of 1.6 was set.

The first case of CRF was designed for the same requirements as the baseline fan, and the results can be found in table 2. However, it was decided to keep the rotational speed of the front rotor limited as to attain a sonic tip. The speed ratio of the CRF, i.e. the ratio between the rotational speed of the front (FR) and the back rotor (BR) was chosen to be 1. This was done for the sake of simplicity and does not represent an optimum design selection. Due to the swirl that the FR imposes to the air and the counter-rotating speed of the BR, the relative Mach number at the tip of the BR was supersonic.

The second case of CRF was designed for different requirements based on a simple preliminary analysis of the influence of the inner FPR and outer FPR on the TSFC, assuming that the rest of the engine parameters remain constant. This analysis was performed with the help of GasTurb™ [15] and resulted in the contour plot shown in figure 8. From the graph it is clear that the baseline fan lies in a region of almost optimum TSFC for the compression capabilities of a single stage fan. Furthermore, no great improvements are observed away from this point, even for large increases in FPR. Nevertheless it was decided to increase the outer FPR for the sake of demonstration of the superior compression capabilities of a CRF if they were needed (for engines with lower BPR). In this case, no initial limitation on the rotational speed was posed, although it was found that due to the swirl input by the FR, the relative air angles at the BR could be unacceptably large. In order to alleviate this adverse phenomenon, it is possible to decrease the speed ratio. However, by doing that, the desired FPR was not obtained. A solution of compromise was considered at the point of outer FPR 1.74 and inner 1.28. Design parameters for this CRF can be found in table 3.

Once the fans were designed, the take-off event was simulated, spanning from the beginning of the ground roll until a distance sufficiently large from the flyover point. The reference aircraft was the Boeing 777-300 performing a take-off profile as shown in figure 9. No cut-back or any technique of noise abatement procedure were applied. The difference between the pitch angle and the flight path (angle of attack) was assumed negligible as compared to the flight path angle itself. Especially, due to the possible range of values for the angle of attack, its influence on the directivity pattern term of equation 2 (function F_3) is very small and hence no information about the pitch or angle of attack history is necessary.

The semi-empirical models for the fan noise are applied at each time step. The models need to be applied twice, one after the other, if the case under consideration is a CRF. The spectra obtained for each rotor are then added

Table 1 – Design parameters for the baseline fan.

GE90 cycle design point (ref. [14])	
Inner Fan Pressure Ratio	1.358
Outer Fan Pressure Ratio	1.65 → 1.6
Bypass Ratio	8.2
Corrected Mass Flow (kg/s)	1498.9
LP Spool nominal speed (rpm)	2258

Fan rotor design point values					
	r (m)	κ_1(deg.)	κ_2(deg.)	σ	$M_{1,rel}$
Hub	0.480	23.3	-2.9	2.00	0.81
Mean	1.022	45.8	26.1	1.45	1.07
Tip	1.562	58.2	57.1	0.90	1.42

Table 2 – Design parameters for the CRF of reference performance.

CRF-ref front rotor (FR)design point values					
	r (m)	κ_1(deg.)	κ_2(deg.)	σ	$M_{1,rel}$
Hub	0.469	18.0	-13.9	2.0	0.64
Mean	1.044	38.3	15.3	1.5	0.79
Tip	1.618	54.2	39.0	1.0	1.00
CRF-ref back rotor (BR) design point values					
	r (m)	κ_1(deg.)	κ_2(deg.)	σ	$M_{1,rel}$
Hub	0.566	41.3	29.3	2.0	0.85
Mean	1.092	53.9	43.9	1.5	1.00
Tip	1.618	69.5	56.1	1.0	1.16

Table 3 – Design parameters for the CRF of higher outer fan pressure ratio.

CRF-HP front rotor (FR)design point values					
	r (m)	κ_1(deg.)	κ_2(deg.)	σ	$M_{1,rel}$
Hub	0.487	18.6	-17.6	2.0	0.65
Mean	1.055	38.5	15.4	1.5	0.79
Tip	1.623	54.3	38.5	1.0	1.00
CRF-HP back rotor (BR) design point values					
	r (m)	κ_1(deg.)	κ_2(deg.)	σ	$M_{1,rel}$
Hub	0.568	47.9	7.9	2.0	0.85
Mean	1.096	57.7	40.3	1.5	1.00
Tip	1.623	71.3	55.5	1.0	1.16

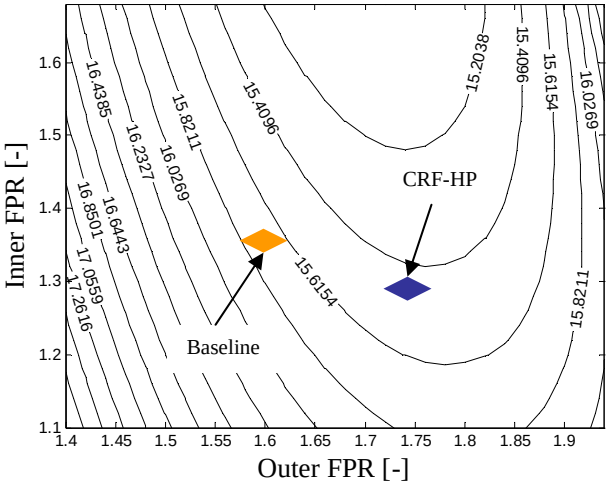

Figure 8 – TSFC contours for varying GE90 inner and outer FPR.

logarithmically. A problem was identified while applying the models to the CRF in series. The rotor-rotor interaction tones occur at a frequency which is not the BPF of the FR, neither the BPF of the BR, but a composition depending on the speed ratio and the number of blades in each rotor. The rotor-alone tones still occur at the BPF of each rotor, unless the tip Mach number is subsonic (no propagation through the duct), which did not happen in any case. On the other hand, the source models predict the tonal noise "all-in-once", because the noise mechanisms generating tones happen at the BPF for a common rotor-stator arrangement. Although modification of the models, or arbitrary introduction of extra tones at rotor-rotor interaction frequencies might be recommended, it was not performed in the present study and the rotor-alone BPF was fed to the models. The FR was indeed considered free of inlet guide vanes (IGV), whilst the FR was considered as IGV to the BR. The input passed to the models at each time step of the take-off simulation is shown in table 4.

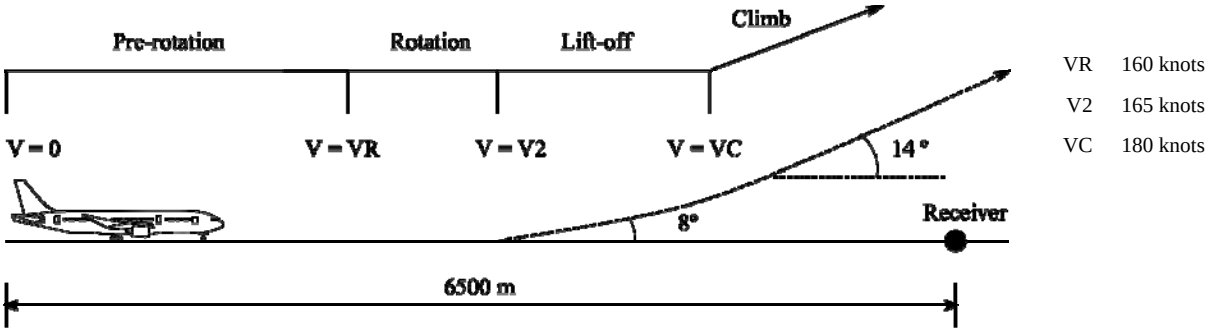

Figure 9 – Take-off profile applied in the present study.

	Baseline	CRF-ref		CRF-HP	
		FR	BR	FR	BR
ΔT_t	39.5	18.3	23.7	18.3	33.0
Corr. Mass	1498.5	1498.5	1498.5	1498.5	1498.5
RPM	2258	1436	1436	1436	1642
Tip Radius	1.56	1.61	1.61	1.61	1.61
Tip Mach	1.42	1.00	1.16	1.00	1.27
Rotor Blades	22	20	28	20	28
OGV/struts	66	28	66	28	66

Table 4 – Fan input for the fan noise source model.

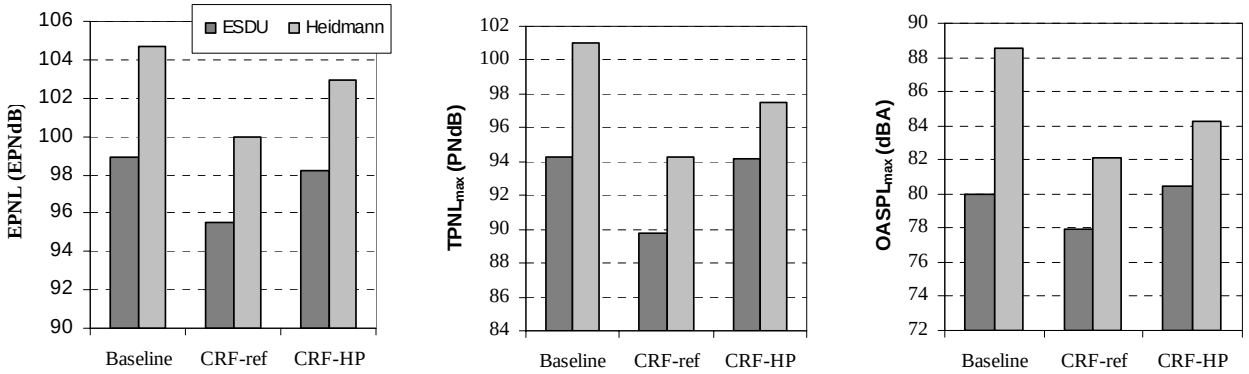

Figure 8 – Results of the simulation at the flyover measurement point.

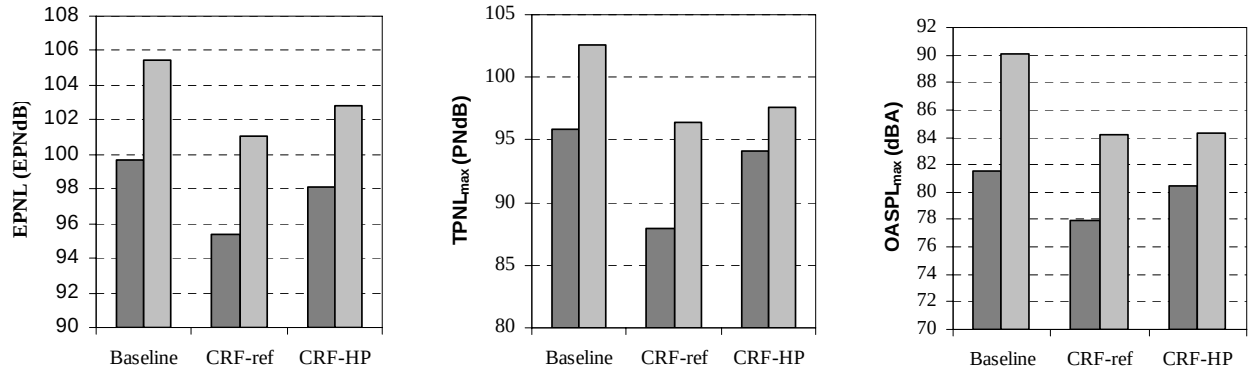

Figure 9 – Results of the simulation at the lateral noise measurement point.

The results for the noise descriptors obtained during the simulation of the take-off with the application of both the Heidmann's method and the ESDU method are shown in figures 8 and 9. It is reminded here that the thrust was kept constant except for the third CRF, which delivers a slightly larger net thrust (1.3%, which has little influence on the fan noise radiation). It is apparent from all the figures that the Heidmann's method predicts larger values for all the noise descriptors at the two measurement positions, this discrepancy being usually large. The results for the lateral noise and the flyover point are also very similar. Due to the steep climbout assumed for the aircraft, this was already at a sufficiently high altitude as not to be influenced much by the extra distance or different emission angle. The EPNL graphs show that the CRF of baseline features is the most silent option during the complete take-off event. The reduction in EPNL is of about 3 EPNdB for both methods. It is also remarkable that the CRF for higher FPR attained EPNL values similar to those of the baseline fan. The same can be said about the maximum TPNL: the use of the CRF of baseline features might result in an annoyance reduction of 2 PNdB. The maximum OASPL shows a reduction of 2 dBA at the flyover point, whereas this reduction can reach values of 4 dBA at the lateral noise measurement point.

4. CONCLUSIONS

This study consisted of several parts: the development of a BEM tool to predict the performance of fan and axial compressors, the development of a reversed BEM tool to be applied for the design of fans, the implementation of semi-empirical source models for fan noise, and the simulation of a take-off event to estimate several noise descriptors. This was to be applied to a baseline GE90 configuration, and two different CRF configuration; one having the same FPR as the baseline engine and another one with higher FPR. Analysis of the results provided some insight into the noise

reduction capabilities of such a novel propulsion concept. The conclusions are:

- No substantial improvements in TSFC were observed by increasing the FPR as compared to the baseline engine case.
- A CRF of similar characteristics to those of the GE90 could reduce the sound level, EPNL, by approximately 3 EPNdB. Similar reductions are expected for the other noise descriptors.
- The CRF of higher pressure ratio is expected to attain noise levels between the baseline and the CRF reference.
- Adaptation of the noise models used seems necessary if the rotor-rotor interaction tones are to be properly captured in the spectrum.
- More elaborate take-off profiles including cut-back, jet noise and atmospheric and ground reflection effects should be implemented for better insight.

REFERENCES

[1] Air Transport Association. *Quarterly Cost Index: U.S. Passenger Airlines*. Website, visited on January, 3rd 2009. http://www.airlines.org/

[2] www.project-vital.com

[3] Lieblein, S., 1965, "Experimental flow in two dimensional cascades", Technical report, Aerodynamic Design of Axial Flow Compressors, NASA SP-36.

[4] Giamati, C.C., Finger, H.B., 1965, "Design velocity distribution in the meridional plane", Technical Report, Aerodynamic Design of Axial Flow Compressors, NACA SP-36.

[5] Schobeiri, M., 2005, Turbomachinery flow physics and dynamic performance, Springer.

[6] Lewis, G., Moore, R., and Kovich, G., 1973 "Performance of a 1.20 pressure ratio STOL at three rotor blade setting angles", NASA. TM-2837.

[7] Moore, R. and Osborn, W., 1979, "Aerodynamic performance of a 1.38-pressure-ratio, variable-pitch fan stage", NASA. TP-1502.

[8] McKenzie, A. B., 1997, " Axial Flow Fans and Compressors: Aerodynamic Design and Performance", Ashgate Publishing Group.

[9] Heidmann, M., 1979, "Interim Prediction method for fan and compressor noise", Technical Memorandum NASA X-71763.

[10] Engineering Society of Data Units, 1998, "Prediction of noise generated by fans and compressors in turbojet and turbofan engines", Data item no. 98008. London, UK. ESDU International plc.

[11] Tyler, J.M. and Sofrin, T.G., 1961, "Axial Flow Compressor Noise Studies, Technical Report, Pratt & Whitney Aircraft Div.

[12] ICAO, 1988, "International Standards and recommended practices, Environmental Protection" Annex 16 to the Convention of International Civil Aviation, Volume I, Aircraft Noise. ICAO, Montreal.

[13] Ruijgrok, G.J.J., 2007, "Elements of aviation acoustics", 2nd Edition, VSSD Delft, The Netherlands

[14] Diwanji, D., Rao, G.A., and van Buijtenen, J.P., 2009, "Feasibility Study of some novel concepts for high-bypass ratio turbofan engines", ASME Turbo Expo 2009. GT2009-59166.

[15] Kurzke, J., 2008, ″Gas Turbine Performance″ http://www.garturb.de.

[16] Cole, J.N, and Kyrazis, D.T., 1956, "A method of calculating the acoustical characteristic of aircraft in flight", Technical Report, Wright Air Development Centre, Wright-Patterson Air Force Base, Dayton, Ohio.